M'hamed DOUMI[1], Abdel Ghani AISSAOUI[2], Ahmed TAHOUR[2], Mohamed ABID[2], and Khalfallah TAHIR[2]

CAOSEE Laboratory, University of Béchar, 08000, Algeria (1), IRECOM Laboratory, University of Sidi Bel Abbes, 22000, Algeria (2)

doi:10.15199/48.2016.03.32

Nonlinear Integral Backstepping Control of Wind Energy Conversion System Based on a Double-Fed Induction Generator

***Abstract**. In this paper, a decoupling control strategy has been applied to control the active and reactive powers generated by a Double Feed Induction Generator (DFIG). We propose a robust nonlinear control based on Backstepping with integral actions in order to control the power of the wind turbine transmitted to the grid and to make the wind turbine adaptable to different constraints. The proposed control laws are derived from the Lyapunov approach which is well suited for this nonlinear system. Furthermore, the proposed integral backstepping control is compared with the classical backstepping controller. The results obtained by simulation prove the effectiveness of the control strategies in terms of decoupling, robustness and dynamic performance for different operating conditions*

Streszczenie.** W artykule opisano strategię sterowania sprzęgania do kontroli mocy czynnej i biernej wytwarzanej przez generator DFIG. Wykorzystano metodę Lapunowa do kontroli turbiny wiatrowej dołączonej do sieci.* ***Nieliniowe sterowanie backstepping do kontroli konwersji energii wiatrowej w generatorze DFIG

Keywords: Double Feed Induction Generator, Robust Nonlinear Control, Lyapunov approach, Integral Backstepping.
Słowa kluczowe: generator DFIG, turbina wiatrowa, metoda Lapunowa.

Introduction

Wind energy is one of the most important and promising source of renewable energy all over the world, mainly because it is considered to be nonpolluting and economically viable. At the same time there has been a rapid development of related wind energy technology [1].

The control of wind energy conversion system (WECS) constitutes a vast subject and is more complex than those of DC drives [2]. Furthermore, Vector control obtains very good application in DFIG because it can allow a decoupling control of the active power and the reactive power. In recent years, many researches of vector control take the following manner to track the largest wind energy under the rated wind speed [1].

Double fed induction generator is widely used for variable-speed generation, and it is one of the most important generators for wind energy conversion systems. Both grid connected and stand-alone operation is feasible [3] through an AC/DC/AC frequency converter [1]. The major advantage of the doubly-fed induction generator, which has made it popular, is that the power electronic equipment has to handle a fraction (20-30%) of the total system power in order to guarantee the stability of the network in acceptable conditions [4].

The DFIG control is based on a stationary model which is submissive to many constraints, such as parameters uncertainties, (temperature, saturation etc.), that might divert the system from its optimal functioning. That is why the regulation should be concerned with the robustness and performances of control techniques [5].

In the last two decades, the backstepping control technique has been widely studied and developed to achieve the stability of the whole system and state estimation problems. This control technique offers good performance in both steady state and transient operations, even in the presence of parameter variations and load torque disturbances. The backstepping control laws are easily constructed and associated to Lyapunov functions [6, 7].

In order to improve the performance and control of the active and reactive powers generated by the DFIG, a robust backstepping controller with integral actions was proposed. The proposed controller exhibits excellent dynamics and steady-state performances.

The objective is to show that the proposed technique can improve performances of doubly-fed induction generators in terms of reference tracking, sensibility to perturbations and robustness against machine parameters variations.

A schematic diagram of a DFIG based wind energy generation system is shown in Fig. 1.

The organization of this paper is as follow: in the second and third sections, we establish respectively the model of the wind turbine and the DFIG. The fourth section is devoted to the control strategy of DFIG. In section 5, the principle of the backstepping control is presented. In sections 6, the integral backstepping control is proposed. The seventh section is devoted to the simulation results and finally conclusions are summarized in the last section.

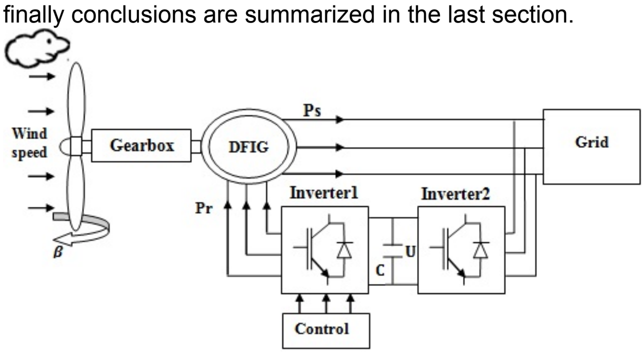

Fig.1. Configuration of DFIG- Wind Turbine

Wind Turbine Model

Wind turbines convert mechanical energy produced by the wind to electrical energy. The mechanical power transferred from the wind to the aerodynamic rotor is

$$P_m = \frac{1}{2}\rho\pi R^2 C_p(\lambda,\beta)v^3 \tag{1}$$

Where ρ is the air density, R is the radius of the wind turbine, v is the speed of the wind, $C_p(\lambda,\beta)$ is the power coefficient, β is the blade pitch angle, and λ is the tip speed ratio of the rotor blade tip speed to the wind speed and is defined by:

$$\lambda = \frac{R\Omega_m}{v} \tag{2}$$

The input torque in the transmission mechanical system is given by the following relation

$$T_m = \frac{P_m}{\Omega_m} = \frac{1}{2\lambda}C_p(\lambda,\beta)\rho\pi R^3 v^2 \tag{3}$$

Where Ω_m is the mechanical speed of the rotor and $C_p(\lambda,\beta)$ is the power coefficient, which expresses the effectiveness of the wind turbine in the transformation of kinetic energy of the wind into mechanical energy.

In the model, the $C_p(\lambda,\beta)$ value of the turbine rotor is approximated using a non-linear function according to [1].

(4) $$C_p(\lambda,\beta)=C_1(\frac{C_2}{\lambda_i}-C_3\beta-C_4)e^{(\frac{C_5}{\lambda_i})}+C_6\lambda$$

With:

(5) $$\frac{1}{\lambda_i}=\frac{1}{\lambda+0.08\beta}-\frac{0.035}{\beta^3+1}$$

C_1=0.5176, C_2=116, C_3=0.4, C_4=5, C_5=21, C_6=0.0068.

The characteristic between C_p and λ for various values of the pitch angle β is shown in Fig. 2. Under certain values of v the wind power can be controlled by adjusting either tip speed ratio or pitch angle. The maximum value of C_p, i.e. C_{pmax}= 0.47, is achieved for β=0 and λ_{opt}=8.15 [1].

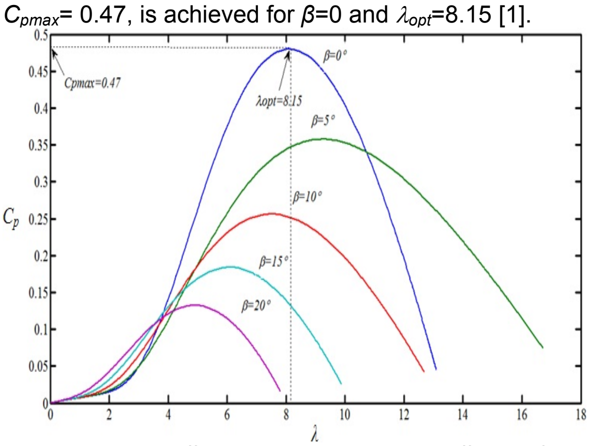

Fig.2. Pitch angle effect on the aerodynamic coefficient of power

Modeling of the DFIG

The modeling of the DFIG is described in the d-q Park reference frame. The following equations systems describe the total generator model [8].

(6) $$\begin{cases} v_{ds}=R_s i_{ds}+\dfrac{d\varphi_{ds}}{dt}-\omega_s\varphi_{qs} \\ v_{qs}=R_s i_{qs}+\dfrac{d\varphi_{qs}}{dt}+\omega_s\varphi_{ds} \\ v_{dr}=R_r i_{dr}+\dfrac{d\varphi_{dr}}{dt}-(\omega_s-\omega_r)\varphi_{qr} \\ v_{qr}=R_r i_{qr}+\dfrac{d\varphi_{qr}}{dt}+(\omega_s-\omega_r)\varphi_{dr} \end{cases}$$

(7) $$\begin{cases} \phi_{ds}=\ell_s i_{ds}+L_m i_{dr} \\ \phi_{qs}=\ell_s i_{qs}+L_m i_{qr} \\ \phi_{dr}=\ell_r i_{dr}+L_m i_{ds} \\ \phi_{qr}=\ell_r i_{qr}+L_m i_{qs} \end{cases}$$

The stator and rotor angular velocities are linked by the following relation: $\omega_s = \omega + \omega_r$.

Equations of electromagnetic torque and motion are:

(8) $$C_{em}=p(\varphi_{ds}i_{qs}-\varphi_{qs}i_{ds})$$

(9) $$C_m-C_{em}=J\cdot\frac{d\Omega}{dt}+f\cdot\Omega$$

The active and reactive powers at the stator provided to the grid are defined by:

(10) $$\begin{cases} P_s=v_{ds}i_{ds}+v_{qs}i_{qs} \\ Q_s=v_{qs}i_{ds}-v_{ds}i_{qs} \end{cases}$$

where: R_s is stator resistence, R_r is rotor resistence, ℓ_s and ℓ_r are respectively stator and rotor inductance, L_m : Mutual inductance, ϕ_{ds} and ϕ_{qs} are respectively direct and quadrature stator flux, ϕ_{dr} and ϕ_{qr} are respectively direct and quadrature rotor flux, i_{ds} and i_{qs} are respectively direct and quadrature stator current, i_{dr} and i_{qr} are respectively direct and quadrature rotor current, p: number of pair poles, ω_s and ω_r: synchronous and rotor angular frequency, respectively, Ω: mechanical angular speed.

Active and reactive DFIG power control Strategy

For obvious reasons of simplifications, the d-q reference frame related to the stator spinning field pattern and the stator flux aligned on the d-axis were adopted. The DFIG is controlled by the rotor voltages. It is an independent control of active and reactive powers [8]. We can write:

(11) $$\begin{cases} \phi_{ds}=\phi_s \\ \phi_{qs}=\dfrac{d\phi_{qs}}{dt}=0 \end{cases}$$

With these conditions the decoupling of torque and flux is guaranteed in the field oriented control and it can be controlled linearly as in the separate excited DC motor [9].

If the per-phase stator resistence is neglected, which is a realistic approximation for medium power machines used in wind energy conversion, the stator voltage vector is consequently in quadrature advance in comparison with the stator flux vector. With these assumptions, the new stator voltages, the fluxes and electromagnetic torque expressions can be written as follows [10, 11]:

(12) $$\begin{cases} v_{ds}=0 \\ v_{qs}=v_s=\omega_s\phi_s \end{cases}$$

(13) $$\begin{cases} \phi_s=\ell_s i_{ds}+L_m i_{dr} \\ 0=\ell_s i_{qs}+L_m i_{qr} \end{cases}$$

(14) $$C_{em}=-p\varphi_s\frac{L_m}{\ell_s}i_{qr}$$

We lead to an uncoupled power control; where, the transversal component i_{qr} of the rotor current controls the active power. The reactive power is controlled by the direct component i_{dr}. The active and reactive powers in the stator and the rotor voltages are given by:

(15) $$\begin{cases} P_s=-v_s\dfrac{L_m}{\ell_s}i_{qr} \\ Q_s=-v_s\dfrac{L_m}{\ell_s}i_{dr}+\dfrac{v_s^2}{\ell_s\omega_s} \end{cases}$$

(16)
$$\begin{cases} v_{dr} = R_r i_{dr} + \ell_r \sigma \dfrac{di_{dr}}{dt} - g\omega_s \ell_r \sigma i_{qr} \\ v_{qr} = R_r i_{qr} + \ell_r \sigma \dfrac{di_{qr}}{dt} + g\omega_s \ell_r \sigma i_{dr} + g\dfrac{L_m v_s}{\ell_s} \end{cases}$$

The total leakage factor σ is given by:

$$\sigma = 1 - \frac{L_m^2}{\ell_s \ell_r} \tag{17}$$

In steady state, the derivative terms in Equation (16) are nil. We can then write:

$$\begin{cases} v_{dr} = R_r i_{dr} - g\omega_s \ell_r \sigma i_{qr} \\ v_{qr} = R_r i_{qr} + g\omega_s \ell_r \sigma i_{dr} + g\dfrac{L_m v_s}{\ell_s} \\ g = \dfrac{\omega_s - \omega_r}{\omega_s} \end{cases} \tag{18}$$

In the same conditions, it appears that the v_{dr} and v_{qr} equations are coupled. We have to introduce a decoupling system, by introducing the compensation terms F_{emd} and F_{emq} in which

$$\begin{cases} F_{emd} = g\omega_s \ell_r \sigma i_{qr} \\ F_{emq} = g\omega_s \ell_r \sigma i_{dr} + g\omega_s \dfrac{L_m v_s}{\omega_s \ell_s} \end{cases} \tag{19}$$

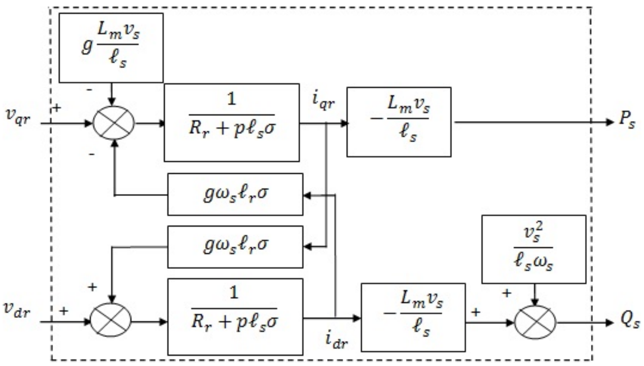

Fig.3. Block Diagram of simplified DFIG model

From Equations (15) and (16), a block diagram containing the rotorique voltages as inputs, and active and reactive statorique powers as outputs, is established in Fig. 3.

Backstepping Control of the DFIG

The backstepping controller mechanism for the active and reactive power regulation have also been applied to the control of generator drives because of their good performances in a wide range of operating conditions. The basic idea of the backstepping control design is the use of the so-called "virtual control" to systematically decompose a complex nonlinear control design problem into simpler and smaller ones. Backstepping control design is divided into various design steps. Each step deals with a single input-single-output design problem, and each step provides a reference for the next design step. The overall stability and performance are achieved by Lyapunov theory for the whole system. The synthesis of this control can be achieved in two successive steps.

Step 1: Computation of the Reference Rotor Currents

In the first step, it is necessary that the system follows given trajectory for each output variable [6]. To do so, a function Y_s^{ref}= (P_s^{ref}, Q_s^{ref}) is defined, where P_s^{ref} and Q_s^{ref} are the active and reactive power references, respectively. The stator active and reactive powers tracking error e_1 and e_3 are defined by:

$$\begin{cases} e_1 = (P_s^{ref} - P_s) \\ e_3 = (Q_s^{ref} - Q_s) \end{cases} \tag{20}$$

The derivative of Equations (20) gives

$$\begin{cases} \dot{e}_1 = (\dot{P}_s^{ref} - \dot{P}_s) \\ \dot{e}_3 = (\dot{Q}_s^{ref} - \dot{Q}_s) \end{cases} \tag{21}$$

Taking its derivative and replacing it in the active and reactive power Equations (15) we get:

$$\begin{cases} \dot{e}_1 = \left(\dot{P}_s^{ref} + v_s \dfrac{L_m}{\ell_s} \dot{i}_{qr} \right) \\ \dot{e}_3 = \left(\dot{Q}_s^{ref} + v_s \dfrac{L_m}{\ell_s} \dot{i}_{dr} \right) \end{cases} \tag{22}$$

In order to check, let us the tracking performances choose the first Lyapunov candidate function V_1 associated to the active and reactive power errors, such us:

$$V_1 = \frac{1}{2}e_1^2 + \frac{1}{2}e_3^2 \tag{23}$$

Using Equations (22), the derivative of Equations (23) is written as follows:

(24)
$$\dot{V}_1 = e_1\left(\dot{P}_s^{ref} + v_s \frac{L_m}{\ell_s} \dot{i}_{qr} \right) + e_3\left(\dot{Q}_s^{ref} + v_s \frac{L_m}{\ell_s} \dot{i}_{dr} \right)$$

This can be rewritten as follows:

$$\dot{V}_1 = -K_1 e_1^2 - K_3 e_3^2 \tag{25}$$

Where K_1, K_3 should be positive parameters, in order to guarantee a stable tracking, which gives:

$$\begin{cases} \dot{e}_1 = (\dot{P}_s^{ref} - \dot{P}_s) = -K_1 e_1 \\ \dot{e}_3 = (\dot{Q}_s^{ref} - \dot{Q}_s) = -K_3 e_3 \end{cases} \tag{26}$$

Equations (26) permits to generate these reference currents assured the Lyapunov stability condition. These currents are given by:

$$i_{dr}^{ref} = \frac{\ell_s}{v_s L_m}\left(-\dot{Q}_s^{ref} - K_3 e_3 \right) \tag{27}$$

$$i_{qr}^{ref} = \frac{\ell_s}{v_s L_m}\left(-\dot{P}_s^{ref} - K_1 e_1 \right) \tag{28}$$

Step 2: Computation of the Reference Rotor Voltages

In this step, an approach to achieve the current references generated by the first step is proposed. Let us recall the current errors, such as:

$$\begin{cases} e_2 = (i_{qr}^{ref} - i_{qr}) \\ e_4 = (i_{dr}^{ref} - i_{dr}) \end{cases} \tag{29}$$

The derivative of Equations (29) gives

(30)
$$\begin{cases} \dot{e}_2 = (\dot{i}_{qr}^{ref} - \dot{i}_{qr}) \\ \dot{e}_4 = (\dot{i}_{dr}^{ref} - \dot{i}_{dr}) \end{cases}$$

Taking its derivative and replacing it in the rotor current references Equations (27) and (28) we get:

(31)
$$\begin{cases} \dot{e}_2 = \left(\dfrac{\ell_s}{v_s L_m}\left(-\dot{P}_s^{ref} - K_3 e_3\right) - \dot{i}_{qr} \right) \\ \dot{e}_4 = \left(\dfrac{\ell_s}{v_s L_m}\left(-\dot{Q}_s^{ref} - K_1 e_1\right) - \dot{i}_{dr} \right) \end{cases}$$

One can notice that Equations (31) include the system inputs: the rotor voltage. These could be found out through the definition of a new Lyapunov function based on the errors of the active, reactive power and of the rotor currents, such that:

(32)
$$V_2 = \frac{1}{2}\left(e_1^2 + e_2^2 + e_3^2 + e_4^2\right)$$

The derivative of Equations (32) is given by:

(33)
$$\dot{V}_2 = e_1\dot{e}_1 + e_2\dot{e}_2 + e_3\dot{e}_3 + e_4\dot{e}_4$$

By setting Equations (31) in Equations (33), one can obtain:

(34)
$$\begin{aligned} \dot{V}_2 &= -K_1 e_1^2 - K_2 e_2^2 - K_3 e_3^2 - K_4 e_4^2 \\ &+ e_2\left(\frac{\ell_s}{v_s L_m}\left(-\dot{P}_s^{ref} - K_1 e_1\right) - \frac{1}{\ell_r \sigma}\left(v_{qr} - R_r i_{qr}\right) + K_2 e_2 \right) \\ &+ e_4\left(\frac{\ell_s}{v_s L_m}\left(-\dot{Q}_s^{ref} - K_3 e_3\right) - \frac{1}{\ell_r \sigma}\left(v_{dr} - R_r i_{dr}\right) + K_4 e_4 \right) \end{aligned}$$

The derivative of the complete Lyapunov function Equations (33) could be negative definite, if the quantities between parentheses in Equations (34), would be chosen equal to zero.

(35)
$$\begin{cases} \dfrac{\ell_s}{v_s L_m}\left(-\dot{Q}_s^{ref} - K_3 e_3\right) - \dfrac{1}{\ell_r \sigma}\left(v_{dr} - R_r i_{dr}\right) + K_4 e_4 = 0 \\ \dfrac{\ell_s}{v_s L_m}\left(-\dot{P}_s^{ref} - K_1 e_1\right) - \dfrac{1}{\ell_r \sigma}\left(v_{qr} - R_r i_{qr}\right) + K_2 e_2 = 0 \end{cases}$$

The rotor voltages then deduced as follows:

(36)
$$\begin{cases} v_{dr} = \ell_r \sigma\left(\dfrac{\ell_s}{v_s L_m}\left(-\dot{Q}_s^{ref} - K_3 e_3\right) + \dfrac{R_r}{\ell_r \sigma} i_{dr} + K_4 e_4 \right) \\ v_{qr} = \ell_r \sigma\left(\dfrac{\ell_s}{v_s L_m}\left(-\dot{P}_s^{ref} - K_1 e_1\right) + \dfrac{R_r}{\ell_r \sigma} i_{qr} + K_2 e_2 \right) \end{cases}$$

where K_2 and K_4 are positive parameters selected to guarantee a faster dynamic of the active, reactive power and rotor current.

In this case, the Lyapunov function derivative is given by:

(37)
$$V_2 = -K_1 e_1^2 - K_2 e_2^2 - K_3 e_3^2 - K_4 e_4^2 \le 0$$

Backstepping Algorithm with Integral Action

The controller is design based on a modified backstepping technique, in order to ensure a high precision control and guarantee high performance power tracking, even in the presence of parameter variations and load torque disturbances, an integral action is now introduced in the backstepping control following the technique used for the doubly feed induction generator [12].

The introduction of the integrators into the model will augment the model of two states. We starts by deriving once the Equations (16) and by introducing the new state variables of i_q and i_d, we obtains the new augmented model:

(38)
$$\begin{cases} \dfrac{di_{dr}}{dt} = i_d \Rightarrow \dfrac{di_d}{dt} = \dfrac{d}{dt}\left(-\dfrac{R_r}{\ell_r \sigma} i_{dr} \right) + w_d \\ \dfrac{di_{qr}}{dt} = i_q \Rightarrow \dfrac{di_q}{dt} = \dfrac{d}{dt}\left(-\dfrac{R_r}{\ell_r \sigma} i_{qr} \right) + w_q \end{cases}$$

The application of the backstepping in this new model allows calculating the virtual control w_q and w_d. They are given by

(39)
$$\begin{cases} w_d = \dfrac{d}{dt}\left(\dfrac{\ell_s}{v_s L_m}\left(-\dot{Q}_s^{ref} - K_3 e_3\right) + \dfrac{R_r}{\ell_r \sigma} i_{dr} + K_4 e_4 \right) \\ \quad + K_6 e_6 + e_4 \\ w_q = \dfrac{d}{dt}\left(\dfrac{\ell_s}{v_s L_m}\left(-\dot{P}_s^{ref} - K_1 e_1\right) + \dfrac{R_r}{\ell_r \sigma} i_{qr} + K_2 e_2 \right) \\ \quad + K_5 e_5 + e_2 \end{cases}$$

This allows a simple integration to return to v_{dr} and v_{qr}, so written as:

(40)
$$\begin{cases} v_{dr} = \ell_r \sigma \int w_d dt \\ v_{qr} = \ell_r \sigma \int w_q dt \end{cases}$$

(41)
$$v_{dr} = v_{dr0} + K_6 \int e_6 dt + \int e_4 dt$$

(42)
$$v_{qr} = v_{qr0} + K_5 \int e_5 dt + \int e_2 dt$$

Where e_5 and e_6 is given by:

(43)
$$\begin{cases} e_5 = (i_{qr}^{ref} - i_q) \\ \quad = \dfrac{\ell_s}{v_s L_m}\left(-\dot{P}_s^{ref} - K_1 e_1\right) + \dfrac{R_r}{\ell_r \sigma} i_{qr} + K_2 e_2 \\ e_6 = (i_{dr}^{ref} - i_d) \\ \quad = \dfrac{\ell_s}{v_s L_m}\left(-\dot{Q}_s^{ref} - K_3 e_3\right) + \dfrac{R_r}{\ell_r \sigma} i_{dr} + K_4 e_4 \end{cases}$$

with choices of $K_5 > 0$, $K_6 > 0$.

The voltages components v_{qr0}, v_{dr0} that appear in Equations (41) and (42) represents the classical version of the backstepping controller. Finally, the proposed control law can be shown in the Fig. 4.

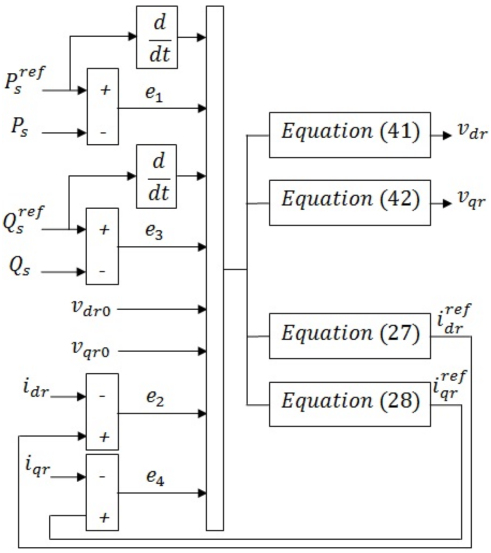

Fig.4. Bloc diagram of the nonlinear integral backstepping control

Results and Discussion

In order to verify the effectiveness of the proposed nonlinear control scheme applied to the DFIG. A bloc diagram is proposed in Fig. 5 to control the whole system.

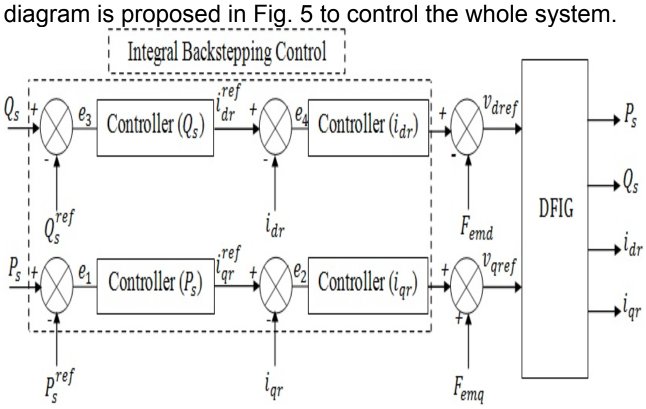

Fig.5. Bloc diagram of the whole system

In this section simulation results are obtained by using the MATLAB/Simulink platform and are presented to show dynamic performances of the control system described above. Controllers will be tested in reference tracking and robustness against parameter variations. The parameters of the induction generator used are given in Appendix.

Reference tracking

The active-reactive stator power and its reference are reported in Fig. 6 and 7. These figures represent a good pursuit, and a perfect decoupling between them is assured, the static error goes to zero, and the time of transient state is so short.

Robustness

In order to test the robustness of the two controllers, the value of rotor resistence R_r is doubled from its nominal value, and the value of mutual inductance L_m is decreased by 10% of its nominal value. Fig. 8, 9, 10 and 11, show the effect of parameter variations on the active and reactive power response for the two controllers.

These results show that parameters variations of the DFIG don't have an observable effect on the powers curves and that the effect proves more significant for classical backstepping controller than that with integral backstepping one. This result enables us to conclude that this proposed control type is more robust.

Basing on all these results we conclude that in term of robustness, integral backstepping technique is more robust compared to the classical backstepping technique.

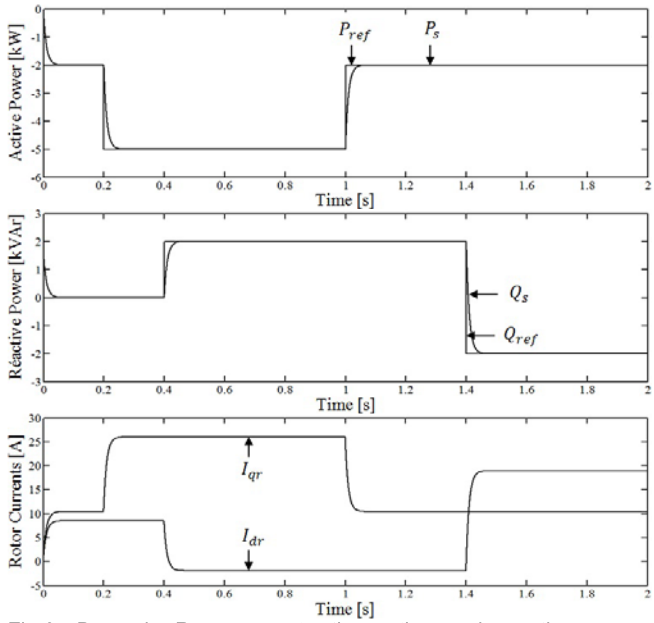

Fig.6. Dynamic Responses to the active and reactive power tracking change using classical backstepping controllers

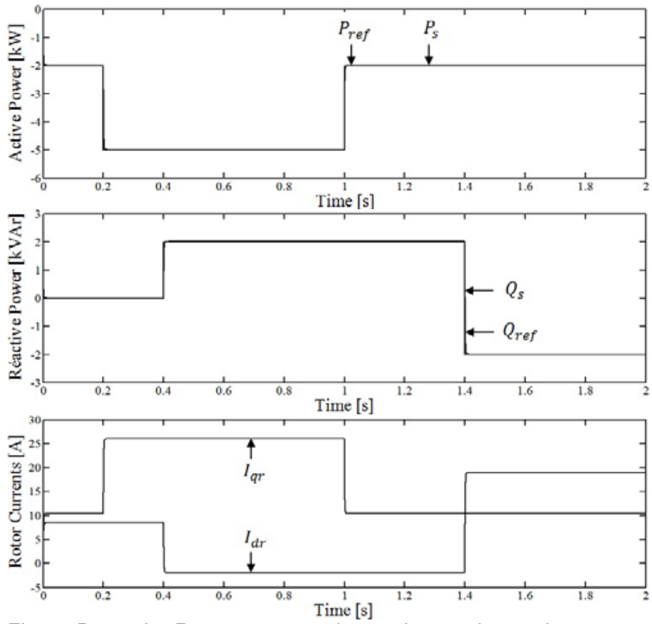

Fig.7. Dynamic Responses to the active and reactive power tracking change using integral backstepping controllers

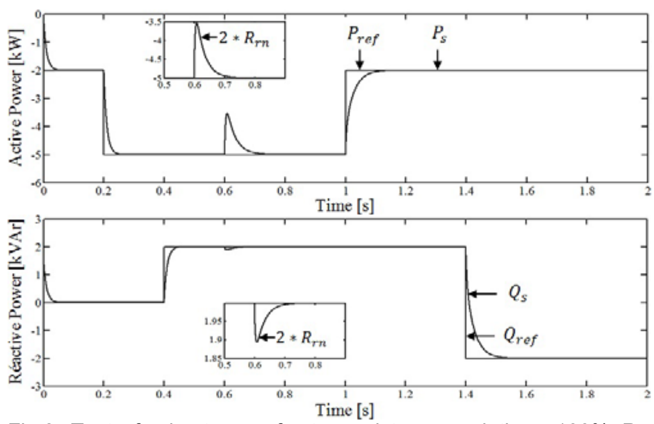

Fig.8. Test of robustness of rotor resistence variation +100% R_{rn} using classical backstepping controllers

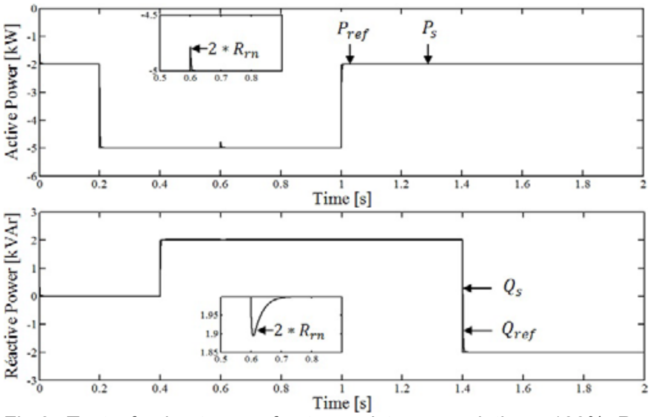

Fig.9. Test of robustness of rotor resistence variation +100% R_m using integral backstepping controllers

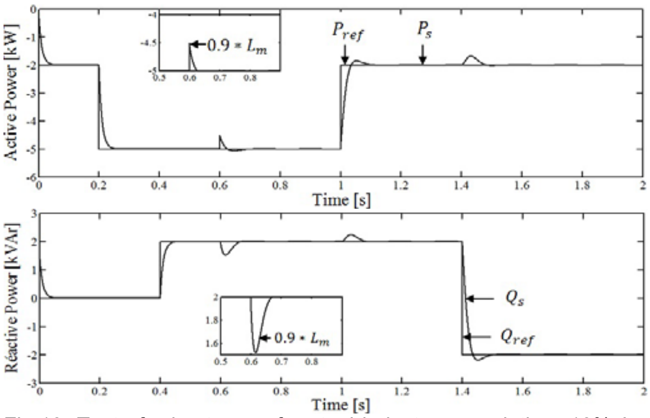

Fig.10. Test of robustness of mutual inductance variation -10% L_m using classical backstepping controllers

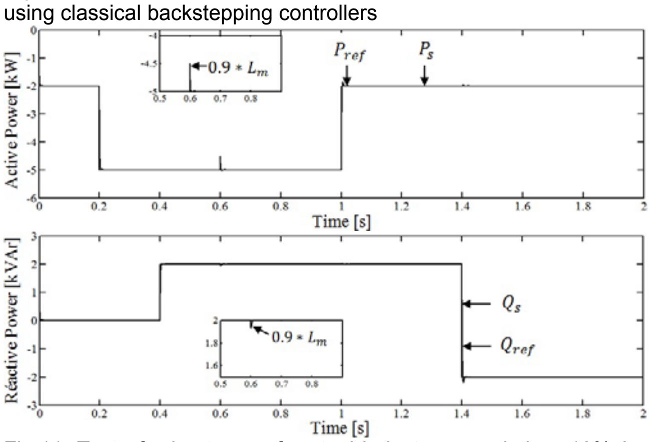

Fig.11. Test of robustness of mutual inductance variation -10% L_m using integral backstepping controllers

Conclusion

This paper proposes a new robust backstepping controller with integral action applied to the wind energy conversion system WECS based on double fed induction generator DFIG. Global asymptotic stability was achieved via the Lyapunov stability analysis. We have developed a decoupling control method of active and reactive powers generated by DFIG.

The main objective of the proposed control method is to ensure of the high performance and a better execution of the DFIG, and to make the system insensible with the external disturbances and the parametric variations.

In term of power reference tracking with the DFIG in ideal conditions, the performances of the two controllers are almost similar. Additionally, the proposed strategy shows a good dynamic performance and ability to reduce the effect of the robustness and hence it is called as robust integral backstepping Control.

Appendix

Rated data of the simulated doubly fed induction generator: 7.5 kW, v_s=220V, F_s=50 Hz, p=3, J=0.1kg/m^2, f=0.06N.m.s/rad, R_s=0.95Ω R_r=1.8Ω, L_m=0.082H, ℓ_s =0.094H, ℓ_r =0.088H.

Acknowledgement

The authors would like to acknowledge the financial support of the Algeria's Ministry of Higher Education and Scientific Research.

***Authors**: M'Hamed doumi, PhD student, Control, Analyzes and Optimization of the Systems Magnet-Energetic Laboratory, Faculty of science & Technology, Electrical Engineering Department, Bechar University, BP 417, Route Kenadsa-Béchar 08000 Algeria, E-mail: doumicanada@gmail.com; Professor Abdel Ghani aissaoui, Interaction Réseaux Electrique-Convertisseurs Machines Laboratory, Faculty of Engineer Science, Electrical Engineering Department, University of Djillali Liabes, BP 98 Sidi Bel-Abbès 22000 Algeria, E-mail: ırecom_aissaoui@yahoo.fr; Ahmed tahour, Associate Professor, Department of Technology, University of Mascara, E-mail: tahourahmed@yahoo.fr.*

REFERENCES

[1] Lee H. H., Dzung P. Q., Phuong L. M., Khoa L. D., Nhan N. H., A New Fuzzy Logic Approach For Control System Of Wind Turbine With Doubly Fed Induction Generator, *Proc. International Forum on Strategic Technology (IFOST)*, Ulsan, South Korea, 13-15 October 2010.

[2] Swagat P., Performance and Power Factor Improvement of Indirect Vector Controlled Cage Induction Generator in Wind Power Application, *Master Thesis*, Dept. of Electrical Engineering, National Institute of Technology, Rourkela, 2011.

[3] Bekakra Y., Ben Attous D., Active and Reactive Power Control of a DFIG with MPPT for Variable Speed Wind Energy Conversion using Sliding Mode Control, *World Academy of Science, Engineering and Technology*, Vol. 5, N°12, 2011.

[4] Payam A. F., Hashemnia M. N., and Faiz J., Robust DTC Control of Doubly-Fed Induction Machines Based on Input-Output Feedback Linearization Using Recurrent Neural Networks, *Journal of Power Electronics*, Vol. 11, No. 5, September 2011.

[5] Ardjoun S. A.E., Abid M., Aissaoui A.G., Naceri A., A robust fuzzy sliding mode control applied to the double fed induction machine, *International Journal Of Circuits, Systems And Signal Processing*, Vol. 5, N°4, 2011.

[6] Trabelsi R., Khedher A., Mimouni M. F., M'sahli F., An Adaptive Backstepping Observer for on-line rotor resistence adaptation, *International Journal of Sciences and Techniques of Automatic control & computer engineering*, IJ-STA, Volume 4, N° 1, July, 2010.

[7] Ullah N., Khan W. and Wang S., High Performance Direct Torque Control of Electrical Aerodynamics Load Simulator using Fractional Calculus, *Acta Polytechnica Hungarica*, Vol. 11, No. 10, 2014.

[8] Abid M., Aissaoui A.G., Ramdani Y., Bounoua H., Sliding Mode Control of A Doubly Fed Induction Generator for Wind Turbines, *Rev. Roum. Sci. Techn. – Électrotechn. Et Énerg*, Vol. 56, N°1, p. 15–24, 2011.

[9] Traoré D., de Leon J., Glumineau A., Sensorless induction motor adaptive observer-backstepping controller: experimental robustness tests on low frequencies benchmark, *IET Control Theory Appl*, Vol. 4, Iss. 10, pp. 1989–2002, 2010.

[10] Boudjema Z., Meroufel A., Amari A., Robust Control of a Doubly Fed Induction Generator (DFIG) Fed by a Direct AC-AC Converter, *Przegląd Elektrotechniczny*, ISSN 0033-2097, R. 88 NR 12a/2012.

[11] Radmehr M., Radmehr M., Amirkhan S., Kalman Filter Based Controller Design for Wind Energy Conversion, *Przegląd Elektrotechniczny*, ISSN 0033 2097, R. 89 NR 2a/2013.

[12] Hamida M. A., Glumineau A., Leon J. d., Robust integral backstepping control for sensorless IPM synchronous motor controller, *Journal of the Franklin Institute 349*, 9 February, 2012.